

Weld Formation Control at Electron Beam Welding with Focal Spot Scanning

¹D.N. Trushnikov ^{2,3}E.G. Koleva, ^{2,3}G.M. Mladenov,
¹V. Ya. Belenkiy and ¹E.S. Salomatova

¹Perm National Research Polytechnic University, 29 Komsomolsky Av.,
Perm, 614990, Russian Federation

²Institute of Electronics Bulgarian Academy of Sciences,
72 Tzarigradsko Chaussee, Sofia 1786, Bulgaria

³Technology Center of Electron Beam and Plasma Technologies,
ul. Vrania 68–70, ap. 10, Sofia 1309, Bulgaria

Abstract: High power concentration in electron beam welding and its deep penetration into metal determine extensive use of electron beam welding (EBW) to produce essential parts from various steels and alloys. The paper covers the issues of non-defect technology development in EBW. The focus mode control issues using the secondary current analysis in the plasma formed above the zone of welding are discussed. Ways to control the formation of the weld with periodic effects on the electron beam (the modulation of the specific beam power) are considered. The statistical analysis of weld geometry is shown.

Key words: Electron Beam Weiding • Focus Regime • Weld Geometry

INTRODUCTION

EBW is a fusion welding process performed in a vacuum. The process has a number of advantages: high power concentration in the electron beam, easy control of the beam energy flow, deeply penetrating beam producing narrow and deep welds, smaller heat-affected zones, equal strengths of the weld joint and the main metal, etc. These advantages allow the use of the electron beam for welding of reactive and non-ferrous metals, high-tensile and heat-resistant alloys that are typically used in the production of critical products.

However, certain problems arise in the EBW process, which are related to the instability of weld-joint formation and the difficulties in controlling the optimal focus regime. The complex character and the lack of understanding of the processes during EBW make numerical modelling difficult, forcing scientists to rely on experimental research methods.

The basic parameters of EBW are accelerating voltage, electron beam current, focusing-coil current, welding speed, operating gun-sample distance, vacuum level in the process chamber, etc. These parameters are chosen according to factors such as the operator's own experience, mathematical models [1, 2], or statistical analysis [3, 4]. The most difficult parameter to identify and reproduce during EBW is the beam focusing position. The operator of an EBW machine needs manually to set the focus of the beam. The adjustment of the focusing-coil current is based on the operator's subjective evaluation of luminosity brightness, emitted from the interaction area of the beam irradiating refractory target material, e.g. wolfram. When the luminosity brightness becomes maximal, the focusing mode is considered sharp [5]. The process of manual focus control is subjective and can lead to performance depreciation. Each operator interprets the luminosity brightness of the operational area differently and, therefore, the welding results may not be reproducible. Changing the focusing current by

1% may cause a 20–60% fluctuation of fusion depth. The focusing position also significantly influences the probability of various defects specific to EBW, such as spiking, cavitations, medial cracks, etc.

The need for real-time focusing control results from changes in the electronic–optical systems of an electronic gun due to cathode wear and tear or after planned maintenance. For welding operation modes, the focusing current should be adjusted based on experiments with various materials, thicknesses and types of electronic-beam guns. Real-time adjustments are important for welding large objects, especially when the cathode electron emission and thus the adjustments of the gun are significant.

Therefore, the control, monitoring and analysis of the processes in the keyhole in the welding bath during EBW requires analysis of the secondary signal parameters, such as secondary electron or ion emission, optical emission, X-rays, etc.

One of the specific processes caused by the impact of the intensive electron beam on the metal during EBW is the formation of plasma in the operational area [6, 7]. The parameters of the plasma are closely connected with the electron beam thermal effect on the metal being welded. In [8, 9], the plasma current parameters are suggested for electron beam focusing control.

The application of focal spot scanning (modulation of the focusing lens current) is the method for control of the keyhole wall instabilities. The low frequency scanning of the focusing current has negative effects on the quality of the weld. Application of high frequency scanning of the focal spot to improve the quality of the welded joint is known. However, its applicability to the operational control of the beam focusing has not been investigated until now.

A simultaneous recording of the deflection coil current or the focusing lens current and the secondary current signals collected by the plasma was realised using both approaches in order to affect the beam energy deposition processes in keyhole.

This article studies the behaviour of the current collected from the plasma, generated in the operational area of the electron beam, when using EBW with focal spot scanning (modulation of the focusing lens current), based on the coherent accumulation method [10-12]. This method can be used to obtain not only amplitude ratios, but also the phase ones, as well as determining how the current signals collected by the plasma are synchronised with the deflection current or the focusing lens signals during EBW. These results on the probability

of the generation of the high frequency component of the non-independent gas discharge current (namely the instabilities of electron emission from the super-heated spots on keyhole walls) can be useful as methods to control the EBW focus position against the parameters of the plasma current.

Experimental Procedure: A ring electrode collector was used to measure the secondary current from the plasma. The collector was located over the welding zone. The collector has a positive potential of 50 V. The loading resistance was 50 Ω . The signal from the collector was registered by a data acquisition system and further processed by a computer. The sampling frequency in the experiments was in a range from 100 kHz to 1 MHz per channel.

During the experiments, samples of chrome-molybdenum steel (0.15% carbon, 5% chrome and around 1% of molybdenum) were welded. The accelerating voltage in all experiments was 60 kV. The welding power was 3 kW and the welding speed was 5 mm/s for experiments of beam oscillations and the welding power was in the range of 2 kW to 4 kW in the case of focusing spot scanning.

During the experiments, the welding power P , welding speed, focus degree ΔI_f ($\Delta I_f = I_f - I_n$ is the difference between the average focusing lens current of the welding mode and the focusing lens current of the sharp focus), the frequency f and the amplitude of the focal spot scanning A were varied.

The current in the focusing or deflection lenses was changed under a linear law. In the case of beam deflection oscillations experiments, the deflection oscillation frequency ranged between 50 Hz and 1,400 Hz and the range of the duplicated maximal amplitude of the beam deflection oscillation was 0.4 mm to 3.5 mm.

In the case of beam focus scanning, the limits of the scanning frequency were from 90 to 12,000 Hz. The amplitude of these oscillations was in the range of 3 to 25 mA.

Transverse metallurgical sections of the weld were made from all the welded samples. The focus regime was determined by the transverse sizes of the penetration depth. The sharp focus regime corresponds to the maximum penetration depth.

Measured Results: Fig. 1 shows a typical spectrum of the secondary current signal collected from plasma during the welding of steel samples. It can be noted that there is the same characteristic maximum in the signal at frequencies

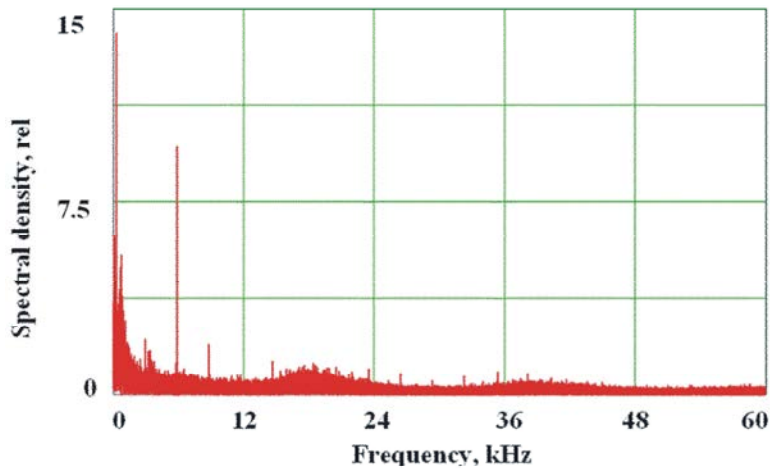


Fig. 1: A typical signal spectrum of the secondary current collected from the plasma during EBW with focus position oscillation (welding power: 2.5 kW, sharp focus regime ($\Delta I_r=0$), scanning frequency: 1,523 Hz).

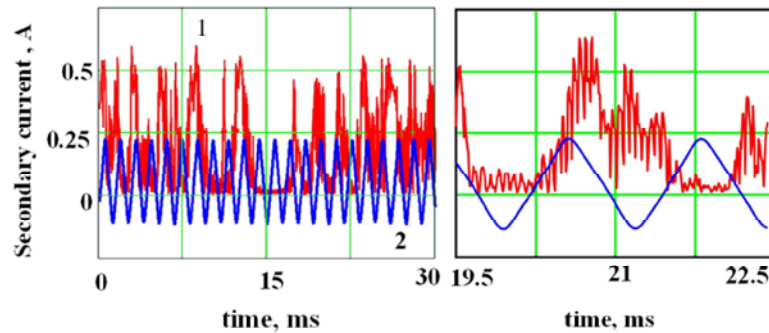


Fig. 2: Waveform of secondary current, collected from the plasma and the signal of the focus coil current during EBW with focus position oscillation: 1. Secondary current. 2. Signal from the focusing lens current.

close to 15–20 kHz. The collected from the plasma signal record (Fig. 2) looks like a series of high frequency impulses that follow each other (curve 1). For comparison, the record of deflection oscillations current (curve 2) is shown. The impulses of the series of the secondary signal appear with frequency of order 10–30 kHz and have considerable values (impulses value depends on the current selection conditions and reached 1 A in the performed experiments).

The similarity of these records of the high frequency current signals, collected by the plasma at periodic interaction on beam energy absorption in the keyhole in the welding bath, can be seen. There is a hypothesis to explain the mechanism of the appearance of high frequency oscillations in the collected current by the positive electrode in the plasma. The collector plays the role of an anode in a non-independent discharge. The plasma in the keyhole and the plasma plume over the interaction zone is an electrically conductive media in that discharge. The electron emission occurs from over-heated

spots on the walls or in the bottom part of the keyhole. These spots are explained with the assumption of the existence of electron beam ablation (explosive boiling) [13–15]. The rate of the energy input in the interaction zone of the electron beam with the metal in the keyhole is much higher than the rate of heat removal through conduction. There is local over-heating of the metal, followed by explosive boiling. The boiling metal vapour affects the beam structure, the local beam part is scattered by the metal vapour and by the blow-up ablation products and the power density is dramatically reduced. After the vapour evacuation from the keyhole, the beam power density is again above the critical and the process resumes. The frequencies predicted by this hypothesis are close to the high frequency component, observed experimentally (Fig. 1 and Fig. 2). The local over-heating of the metal walls of the keyhole is a result of the local areas with lower angle in respect to near to vertical walls of the front side of the keyhole in the welding bath. Some blow-up droplets also absorb additional energy and are

for a short time over-heated. As a result the thermal electron emission from over-heated spots plays the role of an impulse cathode emitter in non-independent gas discharge with an anode – the collector electrode.

In the given work, research into the secondary signal was conducted using coherent accumulation, which is an enhancement of coherent detection and is widely applied to tracking an electronic beam on a seam, but it has been applied to research processes in the keyhole and welding control only recently. In this research, the high-frequency range 15–20 kHz was studied. The small-width square-wave signal is formed from the signal from the current of the focusing lens ($Osc(t)$) - a basic signal $g(t)$. The basic signal $g(t+\tau)$ is shifted relative to the initial signal $Osc(t)$ for a set time τ . The signal of the secondary current, collected from the plasma $I_c(t)$ is processed by a digital or analog high-pass filter with a cutoff frequency around 10 kHz. The selected signal of the high-frequency component ($Data(t)$) is rectified and then multiplied by the basic signal, $g(t+\tau)$. The result is integrated over time. As a result, we have the function $S(\tau)$

$$S(\tau) = \int_0^{t_0} g(t+\tau) \cdot |Data(t)| dt$$

where t_0 is the sampling time. This function $S(\tau)$ expresses the average amplitude of the high-frequency secondary signal for each value of the shift. In other words, for each value of focusing lens current, there is an average value of the amplitude of the high-frequency oscillations of the secondary signal.

Fig. 3a shows the results of processing the secondary current signal using coherent accumulation with focal spot scanning. The underfocus regime was used. The frequency was 966 Hz and the amplitude of the

focusing lens current oscillations was 7 mA. It is possible to present this function in phase space. For this purpose, on a horizontal axis we postpone the current of the focusing lens (Fig. 3b). The characteristic lag of the high-frequency component signal relative to the deflection coil current signal may be noted.

Fig. 4 shows the results when the beam is over-focused. The change in sign of the correlation coefficient when the beam is focused is of major interest. When the beam is under-focused the coefficient's sign is positive. As the focusing current is increased, the coefficient's magnitude decreases monotonically, becoming zero in the region of sharp focus. A similar phenomenon has been observed in the entire range of investigated conditions. The total number of observations in the multi-factor experiment was 107.

The change in the sign of the correlation coefficient during a change in the focusing current is highly significant. The existence of an extreme in the amplitudes of the high-frequency oscillations of the secondary current in the plasma as a function of the focusing current as it is slowly changed may be explained by the existence of an extreme in the welding parameters (weld penetration, width of the melting zone, etc.). In the experiments described, the frequency of change of the focusing current was several orders of magnitude larger than the frequencies characterizing the geometry of the melting zone. The results obtained confirm the hypothesis that the probability of the occurrence of high-frequency oscillations as well as the amplitude of those oscillations in the secondary waveform, increase monotonically given an increase in the concentration of energy in the area of interaction between the electron beam and the metal in the melting zone.

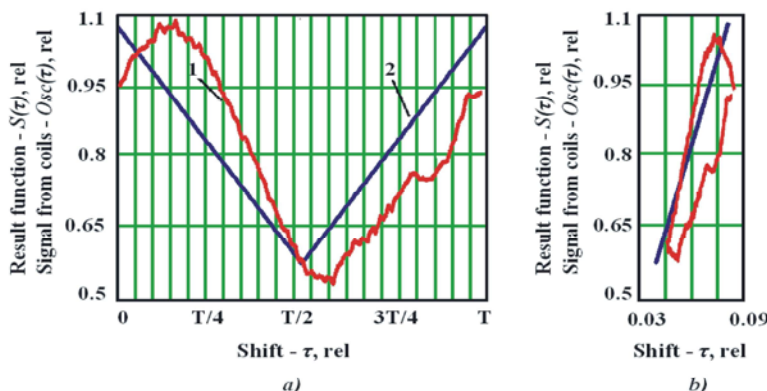


Fig. 3: 1- Function $S(\tau)$, obtained using the coherent accumulation method on τ , is the result of secondary processing of the high-frequency component signal. 2- $Osc(\tau)$ is the record of the focusing lens current ($P=2.5$ kW, underfocus regime ($\Delta I_f = -10$ mA), oscillation frequency $f=966$ Hz).

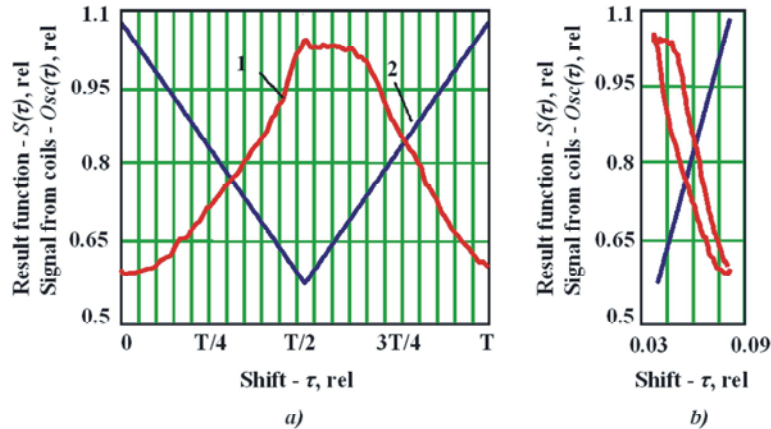


Fig. 4: 1- Function $S(\tau)$, obtained using the coherent accumulation method on τ , is the result of secondary processing of the high-frequency component signal. 2- $Osc(\tau)$ is the record of the focusing lens current ($P=2.5$ kW, overfocus regime ($\Delta I_f = +17$ mA), oscillation frequency $f=966$ Hz).



Fig. 5: Weld cross-section at 35mA beam current, 835mA focusing current and focus scanning: 9mA, 960 Hz $v=5$ mm/s.



Fig. 6: Weld cross-section at 31mA beam current, 826mA no focus scanning, welding velocity 5 mm/s.

It can be concluded that the time shift in the created by coherent accumulation method curves of probability of excitation of high frequency current component $S(\tau)$ could be a base for new control methods for adjustment of the beam focus position during welding with periodic

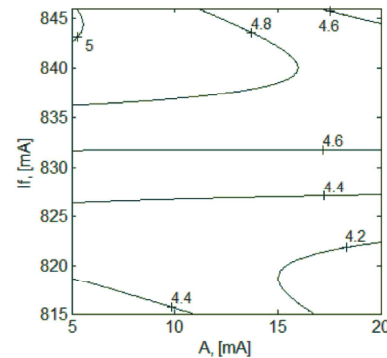


Fig. 7: Contour plot of weld width on surface on A and I_f at focus scanning frequencies $F=1,116.5$ Hz.

interactions on the electron beam (scanning the beam focus). Such method of focus position control, due to monotonic relation of the feedback signal with the focusing lens current, is faster than any known methods, which need the application of an additional focus exploratory scanning.

On the Weld Cross-Section Control: The metallographic cross-sections of the welds, produced by scanning the focusing position along the beam axis, shown on Fig. 5 and Fig. 6. In this case at welding chrome-nickel steel the cross-section has a big head and narrow and deep weld. In some applications a more thick shaft and proportionally smallest head can be acceptable (Fig. 6)

On Fig. 7 is shown contour plot of weld width on surface (namely width of weld-head) on amplitude of scanning and focusing lens current. One can see the same more strong dependence on position of focus on weld

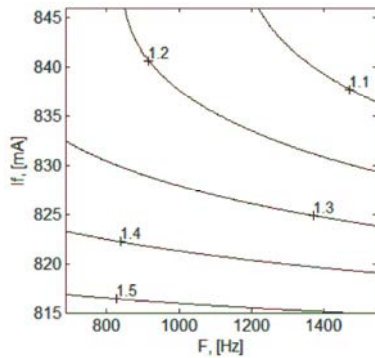


Fig. 8: Contour plot of weld width measured on one-half of the weld depth versus F of focus scanning and focusing current If at scanning amplitude A=12.5 mA

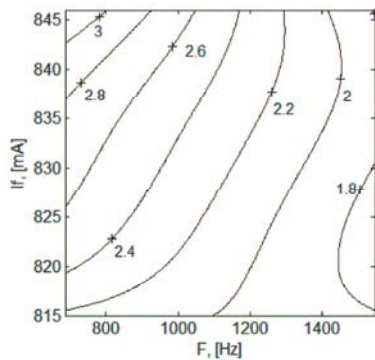


Fig. 9: Dependences of the depth of the weld-head on F of focus scanning and on focusing current If at scanning amplitude A=12.5 mA.

width, as well as that at small amplitudes of focus scanning are the regions of more width welds at down-focused and over-focused beams.

On Fig. 8 is shown the contour plot of weld width, measured on one-half of weld depth on focus scanning frequencies and focusing current at constant scanning amplitude A=12.5 mA. For over-focused beam an increase of scanning frequency decrease of weld width, as well as at down-focused beam the scanning frequency is practically not affects the weld width, measured at one-half of the weld depth.

On Fig. 9 is shown contour plot of the depth of head (more wider upper part of the weld on F of scanning and focusing position at constant amplitudes of scanning and welding speed). Smallest depths of the weld-heads is observable at down-focused beam and higher scanning frequencies.

CONCLUSION

This paper studies the possibility to control processes of beam interactions in the keyhole, situated in the welding bath utilising the plasma current, collected by positively charged ring over zone of beam/sample interaction. The studies are executed at condition of interaction on beam with periodic action (scanning of beam focus position along the beam axis). Welding of chrome-molybdenum and chrome-nickel steels are studied and geometry characteristics of the welds are presented. A new method of control of focusing position at studied condition is proposed.

ACKNOWLEDGEMENTS

This work has been partially carried out with the financial support from the Russian Foundation for Basic Research, research projects No. 11-08-96016-a, No. 13-08-00397A and by Ministry of Education, Perm district, Russian Federation.

REFERENCES

1. Rai, R., P. Burgardt, J.O. Milewski, T.J. Lienert and T. DebRoy, 2009. Heat transfer and fluid flow during EBW of 21Cr-6Ni-9Mn steel and Ti-6Al-4V alloy. *J. Phys. D: Appl. Phys.*, 2(42): 1-12.
2. Rai, R., T.A. Palmer, J.W. Elmer and T. DebRoy, 2009. Heat transfer and fluid flow during EBW of 304L stainless steel alloy. *Weld. J.*, 88: 54-61.
3. Dey, V., D. Kumar Pratihar, G.L. Datta, M.N. Jha and T.K. Bapat, Feb 2009. Optimization of bead geometry in EBW using a Genetic Algorithm. *J. of Mat. Proc. Tech.*, 3(209): 1151-7.
4. Koleva, E., 2005. Electron beam weld parameters and thermal efficiency improvement. *Vacuum*, 11(77): 413-21.
5. Recommended practices for EBW, 1999. Miami, FL: ANSI/AWS, American Welding Society, pp: 1-99.
6. Krinberg, I.A. and G.M. Mladenov, 2005. Formation and expansion of the plasma column under electron beam-metal interaction. *Vacuum*, 77: 407-11.
7. Trushnikov, D.N., V.Ya. Belen'kiy, V.M. Yazovskikh and L.N. Krotov, 2007. Formation of a secondary-emission signal in EBW with continuous penetration. *Weld. Int.*, 5(21): 384-6.

8. Yazovskikh, V.M., D.N. Trushnikov and V. Ya. Belen'kiy, 2004. The mechanism of secondary emission processes in EBW with the modulation of the electron beam. *Weld. Int.*, 9(18): 724-9.
9. Trushnikov, D.N., 2012. Using the wavelet analysis of secondary current signals for investigating and controlling EBW. *Weld. Int.*
10. Max, J., 1981. Méthodes et techniques de traitement du signal et applications aux mesures physiques. Paris: Jean-Louis Lacoume, pp: 10-50.
11. Orfanidis, S.J., 1996. Optimum Signal Processing. An Introduction. New York: Prentice-Hall, Englewood Cliffs, pp: 5-30.
12. Trushnikov, D., V. Belenkiy, V. Shchavlev, A. Piskunov, A. Abdullin and G. Mladenov, 2012. Plasma charge current for controlling and monitoring EBW with beam oscillation. *Sensors*, 12: 17433-45.
13. Smurov, I.Y., A.A. Uglov, A.M. Lashyn, P. Matteazzi, L. Covelli and V. Tagliaferri, 1991. Modelling of pulse-periodic energy flow action on metallic materials. *Int. J. Heat and Mass Transfer*, 34: 961-71.
14. Kovaleski, S.D., R.M. Gilgenbach, L.K. Ang and Y.Y. Lau, 1998. Dynamics of electron beam ablation of silicon dioxide measured by dye laser resonance absorption photography. *Appl. Phys. Letters*, 18(73): 2576-8.
15. Mueller, G., M. Konijnenberg, G. Kraft and C. Schultheiss, 1995. Deposition by means of pulsed electron beam ablation. in *Science and Technology of thin film*, World Scientific Publ.Co PET LTD.